Environmental Research 250 (2024) 118516

Contents lists available at ScienceDirect

Environmental Research

journal homepage: www.elsevier.com/locate/envres

ENSO effects on the relationship between aerosols and evapotranspiration in the south of the Amazon biome

Rafael Palácios [a,b,*], Daniela Castagna [b], Luzinete Barbosa [b], Adilson P. Souza [b], Breno Imbiriba [a], Cornélio A. Zolin [c], Danielle Nassarden [b], Leilane Duarte [b], Fernando G. Morais [d], Marco A. Franco [e], Glauber Cirino [a], Paulo Kuhn [a], Giordani Sodré [a], Leone Curado [b], João Basso [b], Sérgio Roberto de Paulo [b], Thiago Rodrigues [b,f]

[a] Instituto de Geociências, Universidade Federal do Pará, Belém, PA, 66075-110, Brazil
[b] Instituto de Física, Universidade Federal de Mato Grosso, Cuiabá, MT, 78060-900, Brazil
[c] Empresa Brasileira de Pesquisa Agropecuária (Embrapa), Sinop, MT, 78550-000, Brazil
[d] Instituto de Física, Universidade de São Paulo, São Paulo, SP, 05508-090, Brazil
[e] Instituto de Astronomia, Geofísica e Ciências Atmosféricas, Universidade de São Paulo, São Paulo, SP, 05508-090, Brazil
[f] Instituto de Física, Universidade Federal de Mato Grosso do Sul, Campo Grande, MS, 79070-900, Brazil

ARTICLE INFO

Keywords:
ENSO
Aerosol
Evapotranspiration
Topical forest

ABSTRACT

The effects of the El Nino-Southern Oscillation (ENSO) events have local, regional, and global consequences for water regimes, causing floods or extreme drought events. Tropical forests are strongly affected by ENSO, and in the case of the Amazon, its territorial extension allows for a wide variation of these effects. The prolongation of drought events in the Amazon basin contributes to an increase in gas and aerosol particle emissions mainly caused by biomass burning, which in turn alter radiative fluxes and evapotranspiration rates, cyclically interfering with the hydrological regime. The ENSO effects on the interactions between aerosol particles and evapotranspiration is a critical aspect to be systematically investigated. Therefore, this study aimed to evaluate the ENSO effect on a site located on the southern portion of the Amazonian region. In addition to quantifying and testing possible differences between aerosols and evapotranspiration under different ENSO classes (El Niño, La Niña and Neutrality), this study also evaluated possible variations in evapotranspiration as a function of the aerosol load. A highly significant difference was found for air temperature, relative humidity and aerosol load between the El Niño and La Niña classes. For evapotranspiration, significant differences were found for the El Niño and La Niña classes and for El Niño and Neutrality classes. Under the Neutrality class, the aerosol load correlated significantly with evapotranspiration, explaining 20% of the phenomenon. Under the El Niño and La Niña classes, no significant linear correlation was found between aerosol load and evapotranspiration. However, the results showed that for the total data set, there is a positive and significant correlation between aerosol and evapotranspiration. It increases with a quadratic fit, i.e., the aerosol favors evapotranspiration rates up to a certain concentration threshold. The results obtained in this study can help to understand the effects of ENSO events on atmospheric conditions in the southern Amazon basin, in addition to elucidating the role of aerosols in feedback to the water cycle in the region.

1. Introduction

Climate variations that have occurred in recent decades have directly impacted water regimes in the Amazon basin (Marengo and Espinoza, 2016), altering the development of the vegetated surface and causing damage to the forest (Vilanova et al., 2021) and society (Doughty et al., 2015; Gregory et al., 2019). The variability of climatic conditions has produced cycles of deficit and excess rainfall throughout the Amazon region, resulting in extreme drought and floods throughout the basin (Marengo et al., 2013; Brando et al., 2014; Marengo and Espinoza, 2016). Chiang et al. (2021) projects a global increase in the occurrence, intensity, and duration of these extreme events through the next year.

* Corresponding author. Instituto de Geociências, Universidade Federal do Pará, Belém, PA, 66075-110, Brazil.
E-mail address: rpalacios@ufpa.br (R. Palácios).

https://doi.org/10.1016/j.envres.2024.118516
Received 24 November 2023; Received in revised form 8 February 2024; Accepted 16 February 2024
Available online 17 February 2024

Drought events in the Amazon basin have been extensively investigated due to their strong impacts on the ecosystem (Marengo et al., 2013; Sherwood and Fu, 2014; Marengo and Espinoza, 2016; Barkhordarian et al., 2018). Although these studies have assessed the environmental risks, many processes related to the intensity and duration of droughts are still not completely understood (Mishra and Cherkauer, 2010; Zhang et al., 2014). Unlike other extreme weather events, drought involves changes in a broad set of interconnected variables and cannot be attributed to a single factor (Mishra and Cherkauer, 2010). These events, along with aerosol emissions from biomass burning and changes in land use, have fueled and accelerated feedbacks associated with climate change (Davidson et al., 2012; Nobre et al., 2016; Barkhordarian et al., 2019).

El Niño-Southern Oscillation (ENSO) events are responsible for significant variations in the atmospheric circulation patterns (Bonfils et al., 2017; Lu et al., 2018) and consequently in precipitation regimes in the Amazon basin (Barbosa et al., 2019). ENSO is a process composed of two main components, one oceanic (El Niño/La Niña/Neutrality) and another atmospheric (the Southern Oscillation), that occurs on interannual time scales. The oceanic component of ENSO is related to anomalous sea surface temperatures (SST) in the tropical Pacific Ocean. In contrast, its atmospheric component refers to changes in sea level pressures throughout the tropical Pacific basin (Builes-Jaramillo et al., 2023). The ENSO system is further subdivided into two well-defined phases: hot and cold. El Niño is characterized by the abnormal warming of the waters of the Pacific Ocean, while La Niña involves the anomalous cooling of these waters (Lu et al., 2018).

Although several studies have shown the influence of ENSO on climate variables in the Amazon basin (Espinoza et al., 2009, 2011; Davidson et al., 2012; Marengo et al., 2013), there is still a need to investigate relationships between the phenomenon and more complex processes such as those related to climate and agricultural systems (Zhang et al., 2015; Vilanova et al., 2021). Among the properties that still need to be further explored are evapotranspiration and atmospheric aerosols. In particular, these particles interact with solar radiation resulting in positive feedback on evapotranspiration rates through an increase in diffuse radiation (Zhou et al., 2021). In addition, it can interfere in hydrological cycles (Makarieva et al., 2022). Evapotranspiration is a crucial component of the water cycle, and its changes are studied, for instance, for efficient planning of water resources and irrigation control (Zhang et al., 2015).

Due to the vast territorial extension of the Amazon basin, ENSO events can influence specific locations differently, causing more or less severe precipitation anomalies in these locations (Barbosa et al., 2019). These anomalies, associated with changes in air temperature, can locally influence the development of vegetation (Barbosa and Lakshmi Kumar, 2016; Makarieva et al., 2022) and influence changes in aerosol concentrations, generating feedback on the carbon and hydrological cycles (Cirino et al., 2014; Zhou et al., 2021).

Understanding the effect of aerosols on the ecosystem is increasingly necessary, as these particles can affect the productivity of terrestrial ecosystems directly and indirectly (Zhou et al., 2021). Aerosols directly influence gross primary productivity in terrestrial ecosystems, once they interact with solar radiation, increasing the fraction of diffuse radiation that can be used more efficiently for carbon assimilation through photosynthesis (Zhang et al., 2020; Wang et al., 2022). The relationships between aerosols and ecosystem dynamics go beyond carbon fixation rates, as associated with photosynthesis rates. The opening of stomata, for instance, also results in the release of water through transpiration (Zhou et al., 2021; Wang et al., 2022).

Evapotranspiration is regulated mainly by the amount of energy available, that is, by solar radiation. Previous studies by Ramanathan et al. (2001) and Liu et al. (2014) showed that the reduction of this energy due to aerosols and/or clouds causes a decrease in evapotranspiration. However, more recent studies (Lu et al., 2017; Zhang et al., 2021; Zhou et al., 2021; Wang et al., 2022) show that for certain aerosol concentration thresholds, transpiration can be raised, since the increase in diffuse radiation intensifies photosynthesis that stimulates stomatal conductance. Lu et al. (2017) and Zhou et al. (2021) state that aerosols have a negative net effect on evapotranspiration, although they also state that increased transpiration from shaded vegetation for low aerosol loads has a positive effect. Zhang et al. (2020) state that correlations between aerosol and evapotranspiration can be positive or negative depending on the characteristics of the vegetation and the arrangement of leaves. In fact, there are still many uncertainties between the aerosol and evapotranspiration relationship.

For a regional understanding of the relationship between aerosol and evapotranspiration and its possible variations due to ENSO in the Amazon, local studies with reliable measurements of atmospheric conditions over long periods are necessary. In this sense, this study aimed to evaluate the effects of ENSO on evapotranspiration (ET_o) and aerosol load, quantified through the aerosol optical depth (AOD) over a site in the South region of the Amazon basin. In addition, the study also evaluated the long-term variations in ET_o as a function of AOD.

2. Materials and methods

2.1. Site characteristics

Micrometeorological measurements were obtained from an automatic station located at latitude $11°51'42.6"S$, longitude $55°36'45.1"W$ and altitude of 370 m. The station is located within the limits of the experimental area of the Brazilian Agricultural Research Corporation (EMBRAPA) - Agrossilvopastoril, in the municipality of Sinop, Mato Grosso (EMBRAPA, 2023) See Fig. 1. The data were collected between 2014 and 2021. Types of data collected, and sensors used are presented in Table 1.

The EMBRAPA station is located in the Amazon/Cerrado ecotone, presenting vegetation with a diversity of large trees with high canopy density and, twisted and partially deciduous stems (Oliveira et al., 2017; Marques et al., 2020). The region's Köppen climate classification is of the hot and humid tropical (Aw) type, with two marked seasons, classified according to precipitation: rainy (October to April) and dry (May to September), with annual totals between 1800 mm and 2200 mm, and average monthly temperatures above 22 °C (Souza et al., 2013). The rainy season is characterized by having 94% of the annual rainfall, an average temperature of approximately 25 °C, and the lowest global radiation, of 16.44 MJ $m^{-2}.d^{-1}$, which occurs in January. In the dry season, precipitation is around 100 and 200 mm, and the average temperature is 24 °C. This particular period has the greatest thermal amplitude, which is linked to the drecrease of the temperature in June and July, where the monthly averages are of about 22.5 °C, with the radiation reaching 22.75 MJ $m^{-2}.d^{-1}$ (Souza et al., 2013; Zamadei et al., 2021).

2.2. Reference evapotranspiration estimates

Proper estimation of reference evapotranspiration (ET_o) usually requires instrumentation that is usually not available in many sites, especially the ones that measure the total radiation. The non-linear behavior of ET_o makes it hard to be estimated from simple mathematical relationships (Ferreira et al., 2019). However, in a comparison obtained with 21 ET_o models in a Savana site with similar meteorological characteristics to the study area addressed here (Valle Júnior et al., 2020), the best model for the available variables was the one presented in Alexandris and Kerkides (2003), show in Eq. 1

$$ET_o = m_1 + m_2 C_2 + m_3 C_1 + m_4 C_1 C_2, \quad \text{Eq. 1}$$

where ET_o has units of milimiters per day ($mm.d^{-1}$), and with constants given by $m_1 = 0.057$, $m_2 = 0.277$, $m_3 = 0.643$ and $m_4 = 0.0124$.

The variables C_1 and C_2 are directly dependent of average air relative

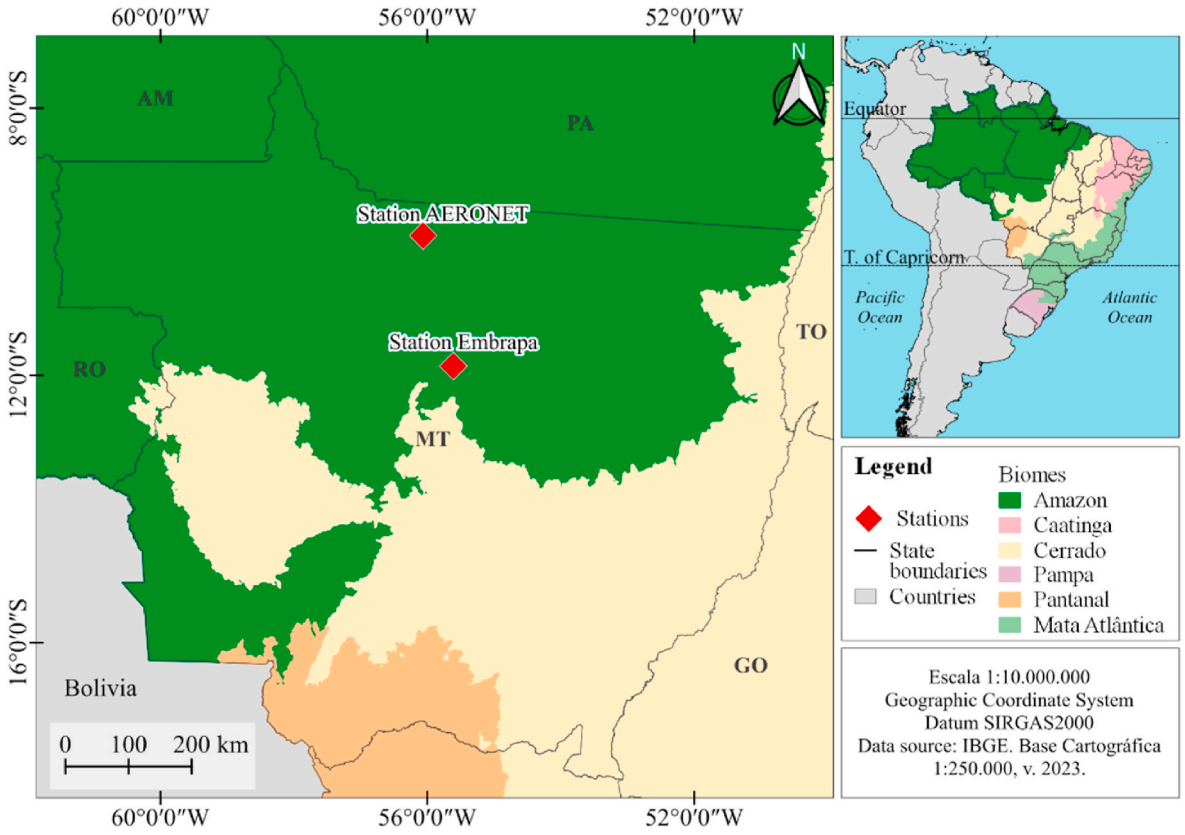

Fig. 1. Geographic location of the measurement stations considered in this study.

Table 1
EMBRAPA automatic station instrumentation and time resolution.

Measurements	Instruments	Temporal resolution
Air Temperature (*T*)	Campbell Scientific, model: HC2S3;	Daily
Precipitation (*PPT*)	Campbell Scientific, model: TB4	Daily
Solar Radiation (*Rs*)	Kipp & Zonen, model: CNR4;	Daily
Relative Humidity (*RH*)	Campbell Scientific, model: HC2S3;	Daily

humidity (*RH*, in %), average air temperature (*T*, in °*C*), and incident solar radiation (*Rs*, in $MJ.m^{-2}.d^{-1}$), given by Eqs. (2) and (3) below:

$$C_1 = 0.6416 - 0.00784RH + 0.372Rs - 0.00264RsRH \quad \text{Eq. 2}$$

$$C_2 = -0.003 + 0.00812T + 0.101Rs - 0.00264RsT \quad \text{Eq. 3}$$

The choice of model considered the best performance for the variables in this study.

2.3. Aerosol measurements

This study used aerosol measurements from NASA's global AERONET network (AErosol RObotic NETwork) (Holben et al., 1998, http://aeronet.gsfc.nasa.gov/), product level 2.0 V3, from the Alta Floresta site (Palácios et al., 2020), approximately 200 km from the EMBRAPA site in Sinop (The "Guide on Meteorological Instruments and Methods" (WMO, 2014), defines a representative spacing between stations to be between 150 and 250 km).

The AERONET measurements used in this work were daily averages of the Aerosol Optical Depth (*AOD*) at 500 nm, the Angstrom Exponent Extinction (*AE*) obtained with the wavelength pair 440–870 nm, and the precipitable water column (*PW*), between 2014 and 2021. As aerosol measurements by AERONET at level 2.0 are not influenced by clouds (Eck et al., 1999; Holben et al., 1998), it is highlighted that throughout the atmospheric column the scale of daily and monthly values leaves little variation for the distance considered in this study. Similar considerations were made in Palácios et al. (2022a).

2.4. Classification of ENSO events

The classification of ENSO events was obtained based on the Oceanic Niño Index (ONI), from the Golden Gate Weather Services digital platform (GGWeather, 2023). Fig. 2 shows the ONI values obtained by quarterly averages.

The ONI values less than or equal to −0.5 are classified as La Niña, the values greater than or equal to 0.5 are classified as El Niño, and those between this interval are classified as Neutrality (Vilanova et al., 2021). With this classification, two well-defined El Niño events are observed, the first between 2015 and 2016 and the second, slightly less intense, between the end of 2018 and 2019. As for La Niña, two events are also clear: between 2017 and 2018 and between 2020 and 2022. In this work, the characteristic year considered for each phenomenon is between August of one year and July of the following year. This choice was associated with the more significant amount of data available for AERONET aerosol analysis.

2.5. Analysis method

After the ET_o calculation, the micrometeorological and aerosol data sets were concatenated into a single file with daily averages. This data set was initially separated according to the ENSO classification: El Niño, La Niña and Neutrality. Subsequently, an analysis of statistical variance was performed to evaluate differences in micrometeorological conditions such as temperature and relative humidity in addition to *AOD* and ET_o.

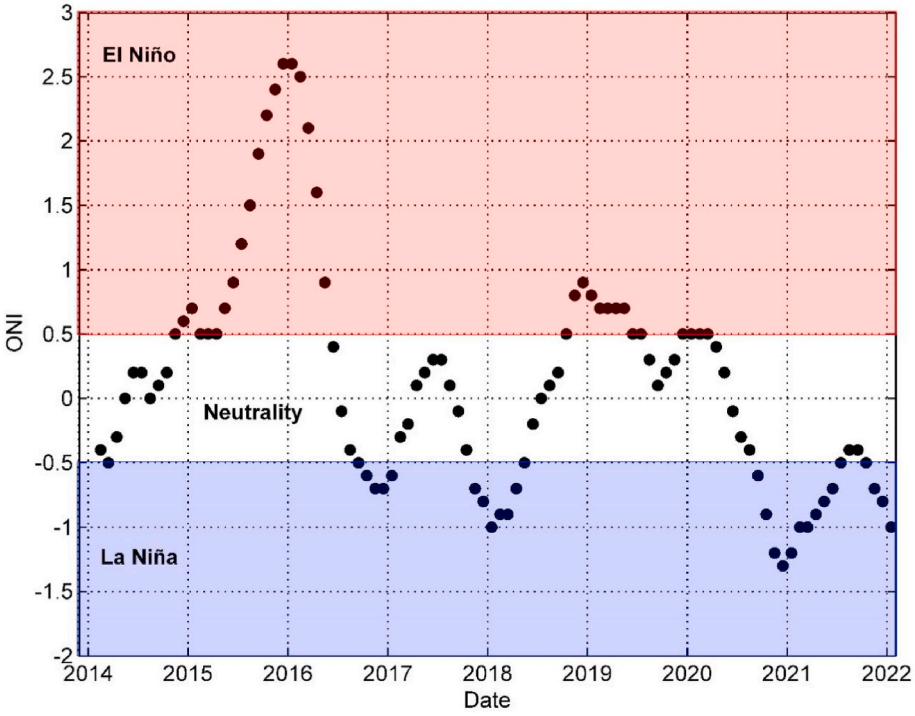

Fig. 2. Classification of El Niño, La Niña, and Neutrality events based on ONI (Oceanic Niño Index) values.

To verify aerosol effects, each ENSO class data set was separated according to *AOD* values. For $AOD \leq 0.10$, a clean atmosphere (clear sky) was considered. For values above this limit, the effects of aerosols were considered. Cirino et al. (2014) carried out a similar discrimination on *AOD* to evaluate aerosols' influence on carbon fluxes. After separation for different atmospheric conditions, the relationship between *AOD* and ET_o was evaluated.

Statistical analysis of the variance with average comparisons were performed using the *t*-test, and the evaluation of differences using the Mann-Whitney, Mood median, Kolmogorov-Smirnov, Anderson-Darling, and Epps-Singleton tests. The differences analyzed were only considered in cases of significant p-value in all tests, such as significant differences for p-value <0.05 and highly significant differences for p-value <0.001. Correlations were evaluated using Pearson's correlation coefficient, of which the significance level was also evaluated in terms of p-value <0.05 and 0.001. Statistical analyses and tests were carried out with the Statsmodels module in Python. Graphical analyses were performed with MatLab computational platform, version R2023b.

3. Results and discussion

3.1. ENSO influence on the local microclimate and aerosol load

Precipitation (*PPT*) in the studied area presents variability similar to the patterns observed in most of the Amazon region, being characterized by two well-defined periods (Marengo et al., 2013; Sousa et al., 2015). Fig. 3 shows that the rainy period occurs between October and April, with February and March the months with the highest volume of precipitation. The dry period occurs between May and September, where July and August are the driest months. In ENSO conditions, fluctuations in precipitation variability were observed. The La Niña phase increases the precipitation a during the rainy season, while the El Niño phase reduces the monthly rainfall. It is worth mentioning that regardless of the ENSO phase, the beginning and end of the rainy and dry periods were not altered, only the total amount of precipitation.

Souza et al. (2013) states that the total monthly and annual rainfall variations are due to the behavior of regional atmospheric circulation

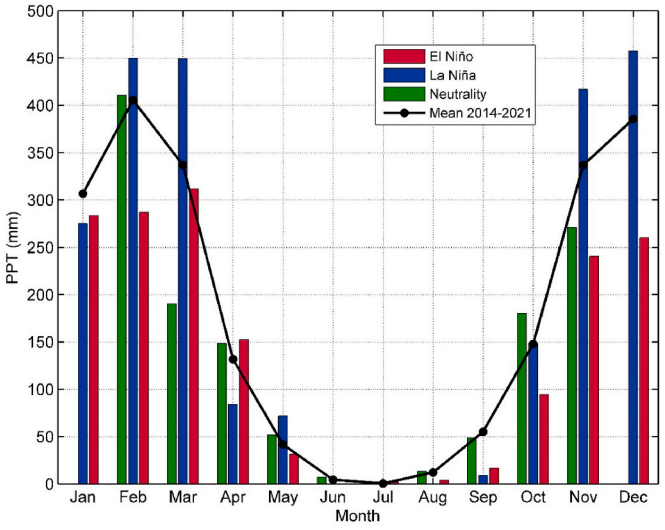

Fig. 3. Monthly accumulated precipitation for characteristic years of El Niño, La Niña and Neutrality, and average precipitation for the studied period (2014–2021).

throughout the year, together with local or regional geographic factors (Barreiro et al., 2002). Carvalho et al. (2002) and Verdan and Silva (2022) indicate that the occurrence of ENSO influences the position of meteorological systems that modulate the rainfall regime in the Brazilian central region, among which the most active in Mato Grosso is the South Atlantic Convergence Zone (SACZ). Thus, the local rainfall can be changed upwards or downwards, mainly due to the position of the SACZ. During the hot phase of ENSO, it becomes more intense in the Amazon southern portion and in the cold phase, it becomes more intense in the Amazon northern portion. These results are in agreement with the rainfall patterns observed in this study.

The variations in *PPT* for the different ENSO classes agree with what

has been reported for other Amazon sites (Espinoza et al., 2009, 2011; Marengo et al., 2013; Sousa et al., 2015; Marengo and Espinoza, 2016). Changes in *PPT* regimes in the Amazon have substantial contributions from meridional variations in the sea surface temperature in the tropical Atlantic (Marengo et al., 2011, 2012). In addition, the accumulated *PPT* in the Amazon is mainly due to large-scale climate systems in the tropical Atlantic (Angelini et al., 2011). Water vapor delivered to the atmosphere through evaporation from forests represents a considerable stock of potential energy (Makarieva et al., 2013), so *PPT* variations throughout the basin are a combination of different processes influenced by large-scale circulation and local processes (Marengo and Espinoza, 2016). Drought events in the Amazon can be associated with atmospheric circulation anomalies due to El Niño, the substantial warming of the tropical Atlantic, or even a combination of both (Aragão et al., 2007).

The variations in the *PPT* depending on the different classes of ENSO are justified by the downward displacement of the Walker cell, directly interfering in the SACZ, over the Amazon. For the El Niño phase, this displacement towards the Brazilian northern region causes an inhibition of convective activities (Pereira et al., 2024), resulting in a *PPT* deficit in the south of the basin. Fig. 3 shows that, in general, the *PPT* for the El Niño is below the average for the study period and that this deficit is more evident in the second semester, in agreement with Souza et al. (2015), Builes-Jaramillo et al. (2023) and Pereira et al. (2024).

Changes in *PPT* regimes are accompanied by variations in atmospheric conditions such as temperature and relative humidity (Marengo and Espinoza, 2016), as shown in Fig. 4. The time series of monthly *PPT* accumulations (Fig. 4d) justifies the variations in *T* and *RH*. Maximum values for *T* occur in all three classes and not just during El Niño. These variations can be attributed to contributions from large-scale circulation from the tropical Atlantic (Angelini et al., 2011). The combination of high temperatures with the extension of the dry period favors the increase in forest fires, considerably increasing the emission of aerosols into the atmosphere (Artaxo et al., 2013, 2022) (Fig. 4e).

For the El Niño class, in comparison to the Neutrality class, the months with the lowest precipitation (June, July, August, and September) showed an increase in the monthly average *T* and a reduction in the average *RH*. During these periods, *T* or the months with the highest precipitation (November, December, January and February), an average monthly increase in *T* was also observed. The increase varied from 0.61 °C in November to 0.94 °C in January, when compared to the periods of neutrality. For the *RH*, there is a decrease ranging from 0.03% in January to 3.71% in November. Under the influence of La Niña, it was observed a clear a decrease in the monthly temperature, ranging from 0.61 °C in June and 0.54 °C in July, when compared to the months of neutrality. Regarding the *RH*, there was a decrease ranging between 1.0% in June and 1.52% in July, compared to the neutral months.

The analysis of *T* on an annual scale revealed higher values in all years affected by El Niño, while, for years characterized by the presence of La Niña, lower values were observed. These results are in agreement with the literature (Moura et al., 2019). According to Jiménez-Muñoz et al. (2016), the El Niño phase caused a record and an extreme drought in the Amazon rainforest during the 2015–2016 period. The phenomenon is one of the main drivers of climate extremes in the Amazon and other tropical regions. Descriptive statistics for *T* and *RH* are shown in Table 2.

The *AOD* time series in 500 nm accompanied by *AE* (*AE* 440–870 nm) (Fig. 5e) highlights the contribution of aerosol emission from fires in the region. Although *AOD* is not a measure of particle concentration, it is a variable that represents the extinction of solar radiation throughout the atmospheric column and is directly proportional to the aerosol load in the atmosphere (Artaxo et al., 2013; Palácios et al., 2020). The *AE* values, which show the spectral dependence of radiation extinction, indicate the aerosol size distribution: the closer to 2.0, the smaller the average diameter of the emitted aerosol. Emissions associated with biomass burning, for the most part, are associated with the fine fraction of aerosols, that is, high *AE* values (Palácios et al., 2020, 2022b).

The time series with daily ET_o values is shown in Fig. 4c. These

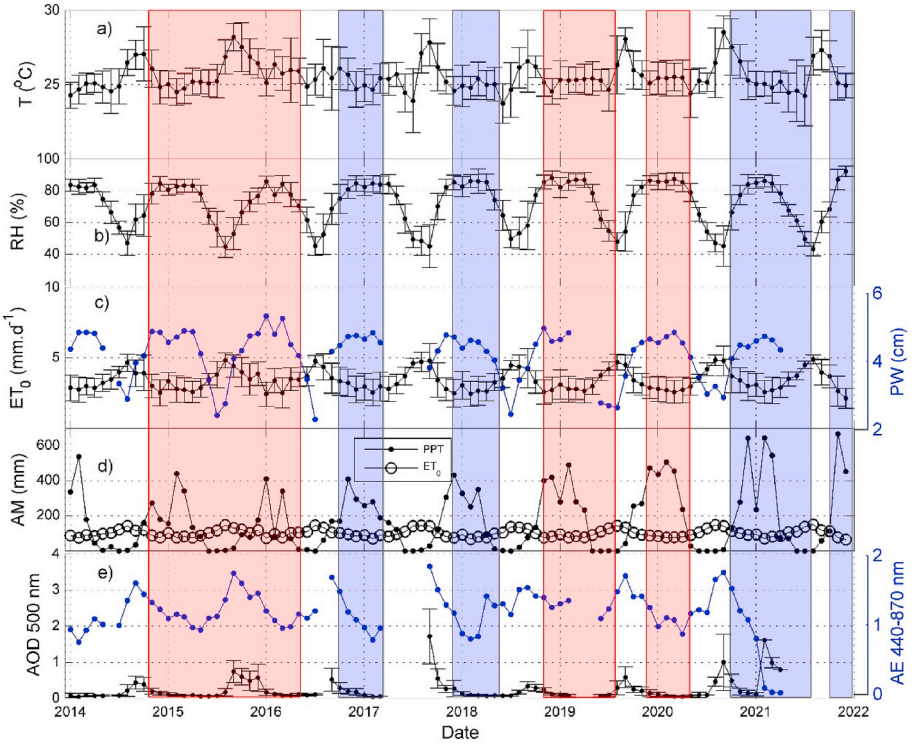

Fig. 4. Time series with monthly averages and deviations for a) *T* (°*C*); b) *RH* (%); c) ET_o (*mm.d*$^{-1}$); d) Monthly accumulated *PPT* and ET_o (*mm.month*$^{-1}$); e) *AOD* 500 nm. In c), the second y-axis (right in blue) shows the monthly averages for the *PW* column (*cm*), and in e), the second y-axis (right in blue) shows the monthly averages for the *AE* 440–870 nm. Red shades highlight El Niño occurrences, blue shades the La Niña, whereas no color shades highlight Neutrality.

Table 2
Descriptive statistics of the variables analyzed for the different ENSO classes. The last column also shows the average number of fire outbreak records in the State of Mato Grosso for the 12-month periods of each ENSO class (https://queimadas.dgi.inpe.br/queimadas/portal).

		Variables						
	Descriptive	*T (°C)*	*RH (%)*	*AOD* 500 nm	*PW (cm)*	*AE 440–870 nm*	ET_o $(mm.d^{-1})$	Fire
El Niño	N	365	365	195	195	195	365	12
	Mean	25.91	70.00	0.33	4.02	1.32	3.50	2312
	Median	25.77	74.75	0.20	4.29	1.30	3.52	–
	Sd	1.55	14.25	0.31	0.85	0.30	1.04	–
	Max	30.19	90.80	1.86	5.26	2.01	5.95	–
	Min	21.53	34.85	0.02	1.68	0.72	0.88	–
La Niña	N	365	365	202	202	202	365	12
	Mean	25.18	74.09	0.18	3.83	1.33	3.26	1503
	Median	25.24	79.00	0.13	4.05	1.36	3.29	–
	Sd	1.47	15.51	0.11	0.80	0.26	1.10	–
	Max	29.04	99.50	0.60	5.11	1.89	6.16	–
	Min	17.70	34.33	0.04	1.82	0.47	0.48	–
Neutrality	N	365	365	184	184	184	365	12
	Mean	25.41	71.98	0.21	3.98	1.26	3.34	2079
	Median	25.26	76.54	0.12	4.14	1.20	3.42	–
	Sd	1.45	13.72	0.18	0.82	0.31	1.00	–
	Max	29.29	91.80	0.95	5.17	2.01	6.17	–
	Min	19.87	37.10	0.04	1.91	0.52	0.62	–

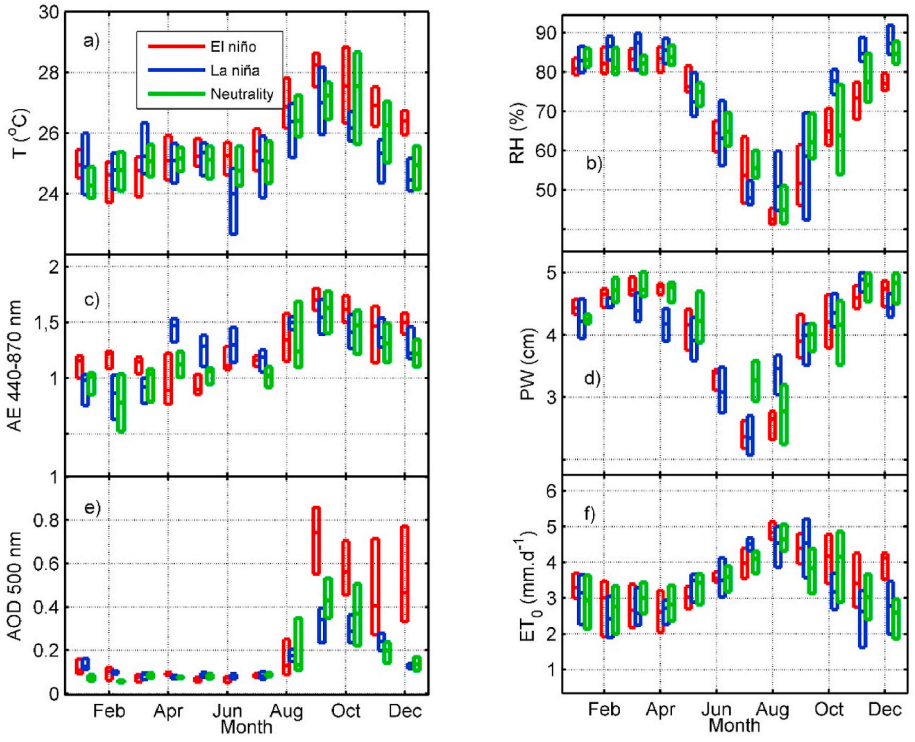

Fig. 5. Comparison of monthly statistics for different ENSO classes. Panels show a) *T* (°*C*), b) *RH* (%), c) *AE* 440–870 nm, d) *PW* (*cm*); e) *AOD* 500 nm and f) ET_o $(mm.d^{-1})$.

values align with results found for a site close to the studied site in the Center-South region of Mato Grosso (Valle Júnior et al., 2020, 2021). Average ET_o values vary between 1.8 and 5.0 mm d^{-1} with recurring maximums at the beginning of the second half of each year, between July and September. The precipitable water column in the atmosphere, *PW* (*cm*), is shown together with ET_o. The *PW* presents evident seasonal variations (Palácios et al., 2020) and an opposite behavior to ET_o. The inverse relationship of *PW* and ET_o can be directly associated with the vapor pressure deficit in the atmosphere. The *PW* is a measure that represents the precipitable water column present in the atmosphere, and, like meteorological variables, it shows a characteristic seasonal behavior, with a maximum in the rainy season and minimum in the dry months (Palácios et al., 2020). The behavior of PW is the opposite to the ET_o. because the water demand for the atmosphere is more intense in the dry season, that is, when the vapor pressure deficit reaches its maximum values and consequently increases the potential to extract water from vegetation (Palácios et al., 2023).

Table 2 also shows the descriptive statistics of *AOD*, *PW*, *AE* and ET_o for the different ENSO classes. The number of observations (*N*) in Table 2 depicts the averages for each day of the year in each class, constituting a characteristic year. Table 2 also shows the average for fire outbreaks (*Fire*) in the state of Mato Grosso for each ENSO class. The differences between the atmospheric parameters for each ENSO class are presented in Fig. 5 and complemented by the analysis of the average

variance shown in Table 3. The temperature monthly distribution (Fig. 5a) shows that, in the year characteristic of El Niño, *T* is lower in the first quarter, with no difference in the second trimester and takes on significant differences from the third quarter onwards when compared to the temperature for the La Niña and Neutrality classes.

When comparing the annual averages for the different ENSO classes (Table 3), a higher temperature was observed during the El Niño phase, where the temperature difference between El Niño and Neutrality was 0.5 °C. The differences between the El Niño and La Niña phases was 0.7 °C, which was shown to be a highly significant difference. For RH, a significant difference was only found between the El Niño and La Niña classes, of around 4.0%.

Although Fig. 5c and d shows wide monthly variations for *AE* and *PW*; a significant difference in *AE* was only found between the Neutrality and La Niña classes and for *PW* only for the El Niño and La Niña classes (Table 3). As for *AOD*, the variations presented in Fig. 5e show (Table 3) a significant difference between practically all ENSO classes. This shows that variations in precipitation regimes (see Fig. 3) for the different classes of ENSO have a significant relationship with the change in the atmospheric aerosol load, verified by differences in *AOD*. However, these differences are not observed for *AE*. This means that regardless of the ENSO classes, aerosols emitted by biomass burning predominate during the dry period.

The average for fire outbreak records in the state of Mato Grosso (see Table 2) in the different ENSO classes shows that for El Niño, there is an increase of close to 10% in relation to the neutrality period. For La Niña, there is an approximate 27% reduction in fire records. Although these numbers represent the average for the entire state of Mato Grosso, it is clear that they contribute strongly to variations in the aerosol optical properties in the study area. The influence of emissions from fires on the *AOD* and *AE* in the southern Amazon basin was evidenced in many studies in the literature (Palácios et al., 2020; Menezes et al., 2018; Morais et al., 2022; Ponczek et al., 2022).

Fig. 5f shows that the variations of ET_o between different ENSO classes are small. However, these differences are statistically significant between the El Niño and Neutrality classes and between El Niño and La Niña, with El Niño phase being the higher in both cases. These differences are likely associated with the influence of aerosols, which can favor, depending on the conditions and emissions, the fertilization of photosynthesis through diffuse radiation (Cirino et al., 2014; Zhou et al., 2021), which contributes to the increased vegetation transpiration rates (Zhou et al., 2021). Another critical issue is that vapor pressure deficit also contributes to transpiration rates, and changing temperature and humidity conditions for the different ENSO classes can affect carbon assimilation through photosynthesis with consequences on ET_o (Palácios et al., 2023). The ET_o increases with the increase in demand for atmospheric water vapor. That is, as the atmosphere becomes drier, the energy available to evaporate water increases, and consequently, ET_o increases (Vilanova et al., 2021). The differences found for ET_o are consistent with the results of Vilanova et al. (2021) on sites in the Western Amazon. Results are also seen for different vegetation cover types, including the savannah type, similar to the cover covered in this study. The results found here suggest, as Costa et al. (2010), that the ET_o for El Niño is higher because combining high temperatures with vapor pressure deficit and radiation availability can control evapotranspiration in tropical forests.

Table 3
Differences obtained by analysis of variances between the different classes of ENSO. Comparison of the mean was performed using the *t*-test, and the evaluation of differences using the Mann-Whitney, Mood median, Kolmogorov-Smirnov, Anderson-Darling, and Epps-Singleton tests.

Mean differences			
Variable	El Niño - Neutrality	El Niño - La Niña	Neutrality - La Niña
T (°C)	0.499[b]	0.732[b]	0.234[a]
RH (%)	−1.203	−4.081[b]	−2.102
AE 440–870 nm	0.061	−0.009	−0.072[a]
PW (cm)	0.045	0.193[a]	0.154
AOD 500 nm	0.126[b]	0.145[b]	0.034[a]
ET_o *(mm/d)*	0.164[a]	0.245[a]	−0.071

[a] p-val <0.05.
[b] p-val <0.001.

3.2. ENSO-AOD- ET_o intercorrelations

The intercorrelations between the studied variables are shown in Table 4 as a correlation matrix. As expected, ET_o had highly significant correlations with *T* and *RH*, regardless of the ENSO class, since these variables were used in the ET_o estimate. For *T*, however, it is observed that the correlation increases as conditions change from La Niña to Neutrality and subsequently to El Niño, where the maximum correlation was $r = 0.73$. Recently, Zhang et al. (2023) showed, through modeling, that *AOD* significantly influences variations in *T*. Globally, *AOD* explains only 3% of these variations. However, on regional or local scales, variations in *T* depending on *AOD* can reach 40%, as was observed for the southern region of India (Zhang et al., 2023). The high aerosol load recorded for El Niño may have influenced *T* variations since the increase in *AOD*, due to local or regional biomass burning (Palácios et al., 2022b), which is associated with emissions of constituents that can scatter or absorb solar radiation (Morais et al., 2022).

The relationships between *AOD* and *T* are cyclical and complex, because the precipitation deficit associated with other meteorological conditions characterize higher temperatures for the El Niño class (Jiménez-Muñoz et al., 2016). However, these conditions are favorable to the increased biomass burning in the region (Palácios et al., 2020; Pereira et al., 2024) and consequently an increase in aerosol emissions (Artaxo et al., 2022). Therefore, it is expected that there will be a positive correlation between *T* and *AOD*. In contrast, the emissions from biomass burning interact with radiation, resulting in an increase in the rate of heating of the atmosphere due to absorption processes (Palácios et al., 2022a; Curado et al., 2023).

The complex part of the analysis consists of determining the fraction of emissions responsible for scattering radiation, which can result in a cooling effect. It can explain the variations in the correlation between *AOD* and *T* for the different classes of ENSO (Table 4), that is, all correlations are significant. However, for El Niño, there is a decrease in the magnitude of the correlation. This decrease is likely associated with the scattered radiation by aerosols during local biomass burning. Curado et al. (2023) analyzed the relationship between maximum air temperatures and fire emissions at a site in the extreme south of the Amazon basin. The correlation found between maximum temperature and the concentration of black carbon (a constituent emitted directly by the burning of biomass) was 0.7. The study justified that this correlation could be even higher if there were no scattering effects of radiation by particles arising from atmospheric transport.

Regarding the *PW* and ET_o variables, it is observed a highly significant inverse correlation in all ENSO classes. This result can contribute to new ET_o estimation models (Spontoni et al., 2023). The correlation between *AE* and ET_o was direct (positive) and, highly significant during El Niño, and significant for the Neutrality and La Niña classes. Although the correlations are low, $r \leq 0.23$, information regarding the aerosol size distribution can be essential in estimating ET_o since the average aerosol size directly influences the scattering rates of solar radiation, impacting ET_o (Zhang et al., 2023).

There was no significant direct correlation for the *AOD* and ET_o variables for the El Niño and La Niña classes (Table 3 and Fig. 6). For Neutrality, there was a positive although low correlation, $r = 0.20$. This result suggests that La Niña aerosol emissions may not impact ET_o rates since, no other adjustment method showed a significant correlation (Fig. 6f). For El Niño, Fig. 6d, shows a direct relationship between *AOD* and ET_o up to *AOD* values close to 0.75. Beyond this limit, there is a possible ET_o saturation and subsequent reduction. This means that the

Table 4
Correlation matrix for different ENSO classes. The number (*N*) of correlated samples corresponded to the availability of aerosol data (El Niño - *N=195*, La Niña - *N=202* and Neutrality - *N=184*).

Correlation matrix							
		T (°C)	*RH (%)*	*AOD* 500 nm	*PW (cm)*	*AE 440–870 nm*	ET_o *(mm.d^{-1})*
El Niño	*T (°C)*	1.00					
	RH (%)	−0.59[b]	1.00				
	AOD 500 nm	0.43[b]	0.08	1.00			
	PW (cm)	−0.06	0.87[b]	0.31[b]	1.00		
	AE 440–870 nm	0.53[b]	−0.19[a]	0.56[b]	0.07	1.00	
	ET_o *(mm.d^{-1})*	**0.73**[b]	**−0.79**[b]	**−0.01**	**−0.54**[b]	**0.23**[b]	1.00
La Niña	*T (°C)*	1.00					
	RH (%)	−0.36[b]	1.00				
	AOD 500 nm	0.34[b]	−0.04	1.00			
	PW (cm)	0.12	0.77[b]	0.32[b]	1.00		
	AE 440–870 nm	0.23[b]	−0.30[b]	0.37[b]	−0.12	1.00	
	ET_o *(mm.d^{-1})*	**0.51**[b]	**−0.86**[b]	**0.03**	**−0.55**[b]	**0.17**[a]	1.00
Neutrality	*T (°C)*	1.00					
	RH (%)	−0.56[b]	1.00				
	AOD 500 nm	0.57[b]	−0.31[b]	1.00			
	PW (cm)	−0.22[a]	0.85[a]	−0.02	1.00		
	AE 440–870 nm	0.45[b]	−0.28[b]	0.69[b]	−0.04	1.00	
	ET_o *(mm.d^{-1})*	**0.67**[b]	**−0.85**[b]	**0.20**[a]	**−0.73**[b]	**0.12**[a]	1.00

[a] p-val <0.05.
[b] p-val <0.001.

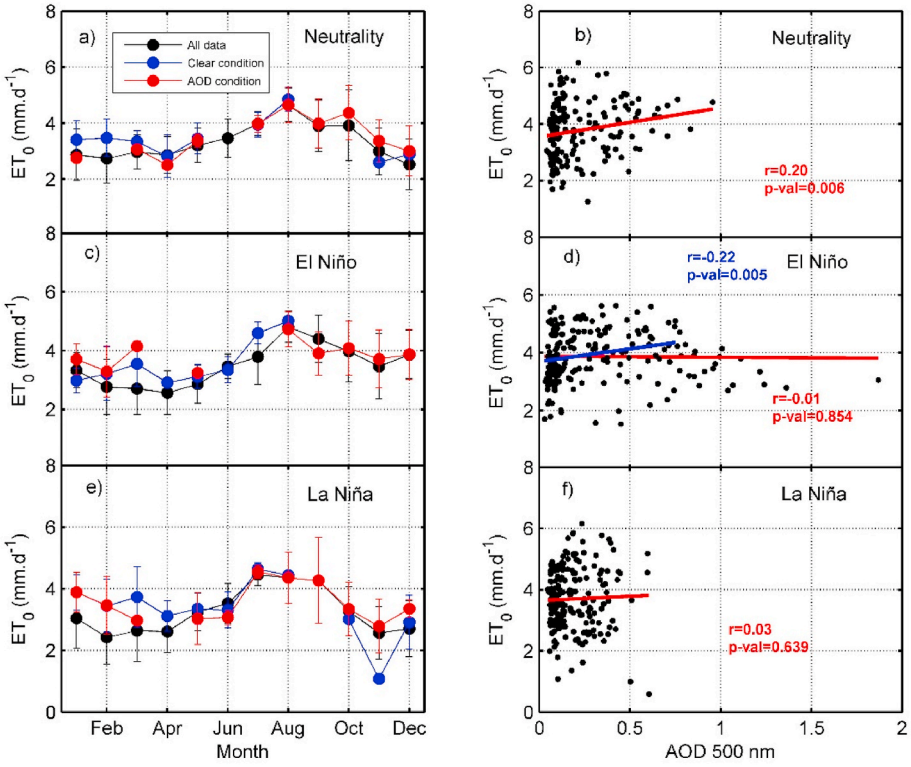

Fig. 6. On the left is a comparison of monthly ET_o statistics under clear sky conditions (blue), presence of aerosols (red), and all data (black) for conditions of a) Neutrality, c) El Niño, e) La Niña. On the right, there is a linear relationship between *AOD* 500 nm and ET_o for conditions of b) Neutrality, d) El Niño, and f) La Niña. All data corresponds to all ET_o estimates, regardless of the ENSO condition, from 2014 to 2021.

processes between aerosols and ET_o are not linear and that more studies are required to unveil these relationships. As for the significant correlation, in the case of Neutrality, we observed that the maximum *AOD* (Fig. 6b) does not exceed 1.0. That is, ET_o may have reached a saturation level but did not pass a limit that causes its reduction.

Fig. 6 (6a, 6c, 6e) also shows the ET_o rates for the ENSO classes, highlighting the influence of aerosols. In these panels, some months do not have ET_o values for *AOD* or clear sky conditions. In these cases, there were no results in the ET_o estimate. Nevertheless, it is possible to observe that for Neutrality (Fig. 6a), the ET_o rates in *AOD* conditions (*AOD* > 0.10) lower than the rates for clear sky conditions in the first half of the year. From the second semester onwards, an inversion occurs, highlighting the possible effect of fire emissions on ET_o rates (Zhou et al., 2021).

For El Niño, starting in September, there are no clear sky conditions. This result confirms that practically all influences of *AOD* on ET_o in this

period can be associated with the emission of local or regional fires (Palácios et al., 2022b). For La Niña, the last quarter of the months (October-November-December) shows a reduction in ET_o rates for clear sky conditions compared to *AOD* and considering all data conditions. In general, Fig. 6 (6a, 6c, 6e) shows that in the second half of the year (July–December), the ET_o maximums are associated with the *AOD* condition, which is evident for all classes of ENSO. However, for El Niño, the *AOD* condition predominates. In addition, Fig. 6 (6b, 6d, 6f) shows that ET_o maxima occur for *AOD* between 0.10 and 0.5 in all ENSO classes, but that for El Niño these maxima are extended for *AOD* up to 0.75.

Fig. 7a shows the monthly averages of relative ET_o and *AOD*, where the relative ET_o is the ratio between ET_o under clear sky conditions ($AOD \leq 0.10$) and ET_o under *AOD* conditions ($AOD > 0.10$) for the entire study period (2014–2021).Fig. 7a also shows the monthly averages for the *AOD*, which visually behave inversely to the relative ET_o. Variations in *AOD*, which occur mainly from August to October, are accompanied by a relative ET_o lower than 1.0, reaching 0.7 in September. That is, for the aerosol emission peak, the fraction of ET_o in *AOD* conditions is higher than in clear sky conditions. Although relative ET_o presents minor variations in the other months, it is observed that for November and December, its values become more significant than 1.0, indicating that ET_o in clear sky conditions is slightly higher in this period. In general, these results suggest that the relationship between *AOD* and ET_o depends directly on emissions from biomass burning, which increase considerably from August to October, in which the fraction of scattering aerosols are predominant (Palácios et al., 2020).

Fig. 7b shows the linear and quadratic relationships between *AOD* and ET_o. A significant correlation was observed for both cases, with a correlation of $r = 0.17$ for the quadratic fit. Although the correlations are low, the aerosol load has a statistically significant influence on ET_o. The linear correlation was lower than previously found for the Neutrality class. However, it shows that, in general, *AOD* correlates positively with ET_o, explaining approximately 10% ($r = 0.10$) of the phenomenon. With the quadratic fit, *AOD* now represents about 17% of the phenomenon, reinforcing that the positive relationship between *AOD* and ET_o has a threshold. The analysis of the quadratic fit curve shows that this threshold for *AOD* is between 0.75 and 1.5. From 1.5 onwards, the curve trend shows a reduction in ET_o as a function of *AOD*.

To verify the influence of local and regional emissions from biomass burning, ET_o was also evaluated as a function of *AE*, with linear and quadratic fit. Fig. 7c shows that the correlation for both adjustments is significant. However, the variation between these fits practically does not differ with *AE* explaining the increase in ET_o by approximately 25%. The relationship between *AE* and *AOD* is also shown in Fig. 7d, where the quadratic fit shows that *AE* maximums occur for *AOD* at up to 1.5, reinforcing the statement of a threshold for *AOD* for positive effects on ET_o rates. The quadratic fit in Fig. 7a shows that for high aerosol loads, the linear correlation between AOD and ET_o is no longer significant, as for *AOD* above 1.5, a reduction in ET_o is observed. For the relationship between *AE* and ET_o (Fig. 7b), the curve fit does not interfere with the direct linear correlation, as the dispersion of radiation by the aerosols positively favors ET_o. In Fig. 7d, both fits represent well the correlation between *AOD* and *AE* (significant linear and quadratic correlation). This is because during biomass burning emissions there is saturation for the *AE* values. Although the aerosol concentration increases, the predominant emissions of aerosols occur and, therefore, for a given *AOD* the *AE* remain constant.

Zhou et al. (2021) highlighted the effects of aerosols on the productivity of terrestrial ecosystems, showing that the effects of aerosols can be both positive and negative, and that these direct and indirect effects significantly impact the development of vegetation. The study found significant positive and negative correlations between *AOD* and gross primary productivity (GPP), depending on vegetation cover. For higher canopy, the correlation values were positive, while for pasture, the results were negative. Zhang et al. (2020) highlight that these correlations depend directly on the phytophysiognomies of the plants, and this helps to understand the results obtained for the south of the Amazon basin. Although the studied area includes a variety of plant species in a transition region between the Amazon biome and the Cerrado, the site is

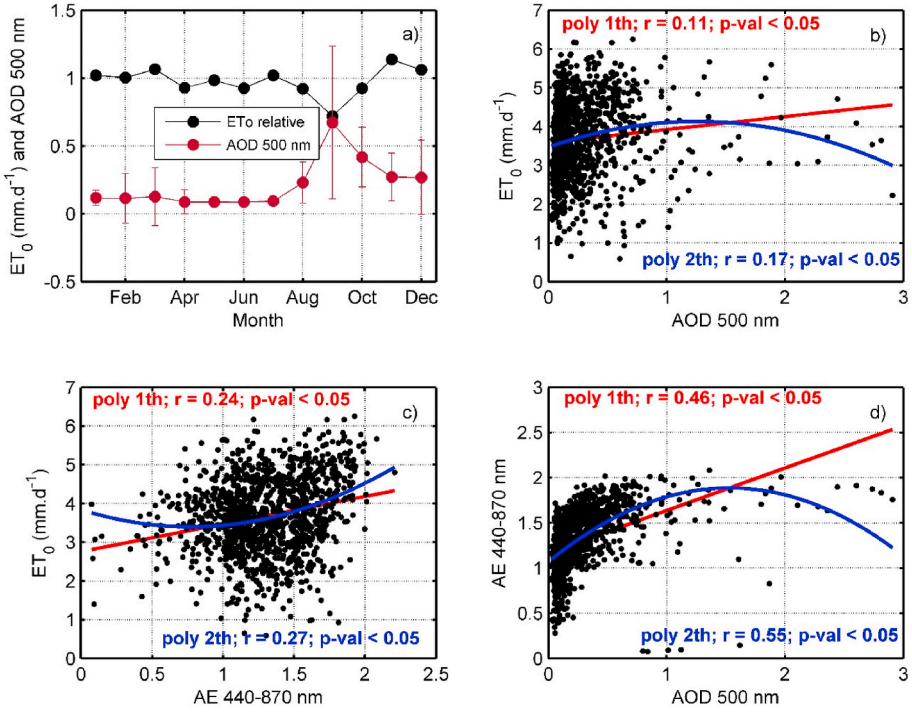

Fig. 7. Relationships of *AOD* 500 nm and ET_o. a) Monthly values of relative ET_o and *AOD* 500 nm; b) Linear and quadratic adjustments between *AOD* 500 nm and ET_o for the entire data series (2014–2021); c) Linear and quadratic fits between *AE* 440–870 nm and ET_o for the entire data series (2014–2021); Linear and quadratic fits between *AOD* 500 nm and *AE* 440–870 nm for entire data series (2014–2021).

composed predominantly of large trees (Vourlitis et al., 2002). Thus, the dispersion of radiation by aerosols can be used more efficiently by shaded leaves below the canopy, favoring ET_o rates.

Lu et al. (2017) and Zhou et al. (2021) state that the net effect of aerosols is negative on ET_o, but the effect of aerosols on radiation can favor transpiration from shaded leaves. The increase in diffuse radiation combined with plants' geometric characteristics and phytophysiognomies can favor ET_o. Therefore, even though there is a negative effect on the top of the canopy due to the interruption of direct radiation, the net result can still be positive (Zhou et al., 2021, 2022; Zhang et al., 2023). The results presented in Fig. 7 show a net positive effect of aerosols, where *AOD* correlates positively with ET_o. However, for high values of *AOD*, this relationship is no longer linear. High aerosol loads can inhibit direct radiation to such an extent that the correlation is no longer positive and significant. This is because the top of the canopy is still responsible for regulating the ET_o of the vegetation.

Although not analyzed in this study, aerosols formed in the atmosphere from emissions from the canopy itself can also influence ET_o rates. Vegetation emits biogenic volatile organic compounds (BVOCs) that are oxidized in the atmosphere, generating secondary organic aerosols (SOA) whose predominance is in the fine mode of the aerosol. The formation of SOA depends on the chemical balance of reactions between BVOC and oxidizing gases in the atmosphere (Liu et al., 2016). These aerosols can also interact with radiation, influencing ET_o rates. However, this relationship would have to be evaluated with chemical measurements in a period free from fires since, during the dry period, the emission from the burning of biomass overlaps the concentration of all-natural constituents in the southern region of the Amazon basin (Artaxo et al., 2013).

The ET_o variations are also influenced by water evaporation from the soil and vegetation, depending mainly on environmental factors such as temperature and relative air humidity (or water vapor deficit), which inhibit photosynthesis and transpiration but favor evaporation (Palácios et al., 2023). In the study presented here, the large fine aerosol load, released from August to October, mostly from local and regional biomass burning events, directly interferes with radiative fluxes through the scattering of solar radiation (Palácios et al., 2020). Consistent with other studies, the effect of aerosols on ET_o found here is positive for small loads but turns negative for values of *AOD* greater than 1.5.

4. Conclusion

This study contributes to new understandings of the effects of ENSO on atmospheric conditions and its implications for the water regime in the south of the Amazon basin. Variations in the *PPT* regime for the different ENSO classes caused significant differences in air temperature, relative air humidity, aerosol load, and ET_o. The evaluation of meteorological conditions for the different classes of ENSO showed that the air temperature is significantly higher in the El Niño condition, with a difference in the annual average of 0.5 °C about the Neutrality condition. Air temperature, in turn, had positive linear correlations with aerosol load (*AOD*) in all ENSO classes. Although there are variations in the magnitude of these correlations, it was found that for El Niño, for a certain *AOD* threshold, this relationship is no longer linear as the scattering fractions can oppose this direct relationship. For *AOD*, a significant difference was also found for the different ENSO classes. We conclude that the prolonged drought caused by El Niño in the region favors the incidence of fires, which considerably increases aerosol emissions with higher *AOD* values.

The combination of analyses between meteorological parameters and aerosol properties allows us to conclude that for the Neutrality condition, there is a statistically significant linear correlation between *AOD* and ET_o. However, this direct correlation is not significant for the El Niño and La Niña classes and the reasons for these results are different. The non-significant correlation for La Niña is due to the low concentration of aerosols, *AOD* below 0.5, with little influence on radiative fluxes. For the El Niño class, a significant positive linear correlation was shown up to a certain *AOD* threshold (~1.0). However, with the increase in *AOD*, this linear relationship ceases to be significant. A significant correlation was between *AE* and ET_o for all classes of ENSO, indicating that fine-mode aerosol emissions favor ET_o in general. We conclude that regardless of concentration, the scattering of radiation caused by fine-mode aerosols favors the dispersion of radiation with positive effects on ET_o rates. We also conclude that the *PW* variable, which had a significant correlation for all ENSO classes ($r > 0.5$ in all ENSO classes) can help in modeling new ET_o estimation methods.

The systemic analysis between *AOD* and ET_o allows us to conclude that the presence of aerosol (*AOD* between 0.10 and 1.5) positively affects ET_o, mainly by contributing to the increase in diffuse radiation. However, for high aerosol loads ($AOD > 1.5$) the reduction of radiation direct sunlight on the top of the vegetation canopy causes a reduction in ET_o. The results shown in this work help to understand the relationships between aerosols and ET_o in the south of the Amazon basin, a region with distinct characteristics of high vegetation. In a future perspective, investigations will be able to elucidate the net effects over the entire extent of the Amazon basin using satellite products or regional models. Still from a future perspective, spatial analysis can contribute to evaluating the relationships between *AOD*, ET_o, and different classes of ENSO in different vegetation covers or biomes. The conclusions shown here can open new perspectives for these analyses.

CRediT authorship contribution statement

Rafael Palácios: Writing – review & editing, Writing – original draft, Formal analysis, Data curation, Conceptualization. **Daniela Castagna:** Methodology, Data curation, Conceptualization. **Luzinete Barbosa:** Methodology, Data curation, Conceptualization. **Adilson P. Souza:** Writing – original draft, Methodology, Data curation. **Breno Imbiriba:** Writing – review & editing, Writing – original draft. **Cornélio A. Zolin:** Methodology, Data curation. **Danielle Nassarden:** Writing – review & editing, Writing – original draft, Data curation, Conceptualization. **Leilane Duarte:** Writing – review & editing, Writing – original draft, Methodology. **Fernando G. Morais:** Writing – review & editing, Writing – original draft, Conceptualization. **Marco A. Franco:** Writing – original draft, Writing – review & editing. **Glauber Cirino:** Writing – review & editing, Writing – original draft, Methodology, Conceptualization. **Paulo Kuhn:** Writing – review & editing, Writing – original draft. **Giordani Sodré:** Writing – review & editing, Writing – review & editing. **Leone Curado:** Writing – review & editing, Writing – review & editing, Conceptualization. **João Basso:** Writing – review & editing, Writing – original draft. **Sérgio Roberto de Paulo:** Writing – review & editing, Writing – original draft, Conceptualization. **Thiago Rodrigues:** Writing – review & editing, Writing – original draft, Conceptualization.

Declaration of competing interest

The authors declare that they have no known competing financial interests or personal relationships that could have appeared to influence the work reported in this paper.

Data availability

Data will be made available on request.

The authors would like to add thanks to the significant contribution from NASA to provide AERONET data (http://aeronet.gsfc.nasa.gov/).

References

Alexandris, S., Kerkides, P., 2003. The new empirical formula for hourly estimations of reference evapotranspiration. Agric. Water Manag. 60, 157–180. https://doi.org/10.1016/S0378-3774(02)00172-5.

Angelini, I.M., Garstang, M., Davis, R.E., Hayden, B., Fitzjarrald, D.R., Legates, D.R., Greco, S., Macko, S., Connors, V., 2011. On the coupling between vegetation and the

atmosphere. Theor. Appl. Climatol. 105, 243–261. https://doi.org/10.1007/s00704-010-0377-5.
Aragão, L.E.O.C., Malhi, Y., Roman-Cuesta, R.M., Saatchin, S., Anderson, L.O., Shimabukuro, Y.E., 2007. Spatial patterns and fire response of recent Amazonian droughts. Geophys. Res. Lett. 34, L07701 https://doi.org/10.1029/2006GL028946.
Artaxo, P., Hansson, H.C., Andreae, M.O., Bäck, J., Alves, E.G., Barbosa, H.M.J., Bender, F., Bourtsoukidis, E., Carbone, S., Chi, J., Decesari, S., Després, V.R., Ditas, F., Ezhova, E., Fuzzi, S., Hasselquist, N.J., Heintzenberg, J., Holanda, B.A., Guenther, A., Hakola, H., Heikkinen, L., Kerminen, V.M., Kontkanen, J., Krejci, R., Kulmala, M., Lavric, J.V., Leeuw, G., Lehtipalo, K., Machado, L.A.T., McFiggans, G., Franco, M.A.M., Meller, B.B., Morais, F.G., Mohr, C., Morgan, W., Nilsson, M.B., Peichl, M., Petäjä, T., Praß, M., Pöhlker, C., Pöhlker, M., Pöschl, U., Von Randow, C., Riipinen, I., Rinne, J., Rizzo, L.V., Rosenfeld, D., Silva Dias, M.A.F., Sogacheva, L., Stier, P., Swietlicki, E., Sörgel, M., Tunved, P., Virkkula, A., Wang, J., Weber, B., Yáñez-Serrano, A.M., Zieger, P., Mikhailov, E., Smith, J.N., Kesselmeier, J., 2022. Tropical and Boreal forest – atmosphere interactions: a review. Tellus B 74, 24–163. https://doi.org/10.16993/tellusb.34.
Artaxo, P., Rizzo, L.V., Brito, J.F., Barbosa, H.M.J., Arana, A., Sena, E.T., Cirino, G.G., Bastos, W., Martin, S.T., Andreae, M.O., 2013. Atmospheric aerosols in Amazonia and land use change: from natural biogenic to biomass burning conditions. Faraday Discuss 165, 203–235. https://doi.org/10.1039/C3FD00052D.
Barbosa, H.A., Lakshmi Kumar, T.V., 2016. Influence of rainfall variability on the vegetation dynamics over Northeastern Brazil. J. Arid Environ. 124, 377–387. https://doi.org/10.1016/j.jaridenv.2015.08.015.
Barbosa, M.L.F., Delgado, R.C., Teodoro, P.E., Pereira, M.G., Correia, T.P., Mendonça, B. A.F., Rodrigues, R.A., 2019. Occurrence of fire foci under different land uses in the State of Amazonas during the 2005 drought. Environ. Dev. Sustain. 21, 2707–2720. https://doi.org/10.1007/s10668-018-0157-4.
Barkhordarian, A., Saatchi, S.S., Behrangi, A., Loikith, P.C., Mechoso, C.R.A., 2019. Recent systematic increase in vapor pressure deficit over tropical south America. Sci. Rep. 9, 15331 https://doi.org/10.1038/s41598-019-51857-8.
Barkhordarian, A., von Storch, H., Zorita, E., Loikith, P.C., Mechoso, C.R., 2018. Observed warming over northern South America has an anthropogenic origin. Clim. Dynam. 51, 1901–1914. https://doi.org/10.1007/s00382-017-3988-z.
Barreiro, M., Chang, P., Saravanan, R., 2002. Variability of the South Atlantic convergence Zone simulated by an atmospheric general circulation model. J. Clim. 15, 745–763. https://doi.org/10.1175/1520-0442(2002)015<0745:VOTSAC>2.0.CO;2.
Bonfils, C., Anderson, G., Santer, B.D., Phillips, T.J., Taylor, K.E., Cuntz, M., Zelinka, M. D., Marvel, K., Cook, B.I., Cvijanovic, I., Durack, P.J., 2017. Competing influences of anthropogenic warming, ENSO, and plant physiology on future terrestrial aridity. J. Clim. 30 (17), 6883–6904. https://doi.org/10.1175/JCLI-D-17-0005.1.
Brando, P.M., Balch, J.K., Nepstad, D.C., Soares-Filho, S., B.S, 2014. Abrupt increases in Amazonian tree mortality due to drought–fire interactions. Biol. Sci. 111 (17), 6347–6352. https://doi.org/10.1073/pnas.1305499111.
Builes-Jaramillo, A., Valencia, J., Salas, H.D., 2023. The influence of the El Niño-Southern Oscillation phase transitions over the northern South America hydroclimate. Atmos. Res. 290, 106786 https://doi.org/10.1016/j.atmosres.2023.106786.
Carvalho, L.M.V., Jones, C., Liebmann, B., 2002. Extreme precipitation events in southeastern south America and large-scale convective patterns in the South Atlantic convergence Zone. J. Clim. 15, 2377–2394. https://doi.org/10.1175/1520-0442(2002)015<2377:EPEISS>2.0.CO;2.
Chiang, F., Mazdiyasni, O., AghaKouchak, A., 2021. Evidence of anthropogenic impacts on global drought frequency, duration, and intensity. Nat. Commun. 12, 2754. https://doi.org/10.1038/s41467-021-22314-w.
Cirino, G.G., Souza, R.A.F., Adams, D.K., Artaxo, P., 2014. The effect of atmospheric aerosol particles and clouds on net ecosystem exchange in the Amazon. Atmos. Chem. Phys. 14, 6523–6543. https://doi.org/10.5194/acp-14-6523-2014.
Costa, M.H., Biajoli, L., Sanches, A.C.M., Malhado, L.R., Hutyra, H.R., da Rocha, H., Aguiar, R.G., de Araujo, A.C., 2010. Atmospheric versus vegetation controls of Amazonian tropical rain forest evapotranspiration: are the wet and seasonally dry main forests any different? J. Geophys. Res. 115, G04021 https://doi.org/10.1029/2009JG001179.
Curado, L.F.A., de Paulo, S.R., da Silva, H.J.A., Palácios, R.P., Marques, J.B., de Paulo, I. J.C., Dalmagro, H.J., Rodrigues, T.R., 2023. Effect of biomass burning emission on carbon assimilation over Brazilian Pantanal. Theor. Appl. Climatol. 155, 999–1006. https://doi.org/10.1007/s00704-023-04673-0.
Davidson, E.A., de Araújo, A.C., Artaxo, P., Balch, J.K., Brown, I.F., Bustamante, M.M.C., Coe, M.T., DeFries, R.S., Keller, M., Longo, M., Munger, J.W., Schroeder, W., Soares-Filho, B.S., Souza Jr., C.M., Wofsy, S.C., 2012. The Amazon basin in transition. Nature 481, 321–328. https://doi.org/10.1038/nature10717.
Doughty, C., Metcalfe, D., Girardin, C., Metcalfe, D.B., Girardin, C.A.J., Farfán Amézquita, F., Galiano Cabrera, D., Huaraca Huasco, W., Silva-Espejo, J.E., Araujo-Murakami, A., da Costa, M.C., Rocha, W., Feldpausch, T.R., Mendoza, A.L.M., da Costa, A.C.L., Meir, P., Phillips, O.L., Malhi, Y., 2015. Drought impact on forest carbon dynamics and fluxes in Amazonia. Nature 519, 78–82. https://doi.org/10.1038/nature14213.
Eck, T.F., Holben, B.N., Reid, J.S., Dubovik, A., Smirnov, O.T.O.N.N., Slutsker, I., Kinne, S., 1999. Wavelength dependence of the optical depth of biomass burning. urban. and desert dust aerosols. J. Geophys. Res. 104, 333–349. https://doi.org/10.1029/1999JD900923.
EMBRAPA, 2023. Empresa Brasileira De Pesquisa Agropecuária Agrossilvipastoril – Estação Meteorológica - Disponível Em. https://www.embrapa.br/agrossilvipastoril/estacao-meteorologica>.Acesso01/08/2023.
Espinoza, J.C., Guyot, J.L., Ronchail, J., Cochonneau, G., Filizola, N., Fraizy, P., Labat, D., de Oliveira, E., Julio Ordonez, J., Vauchel, P., 2009. Contrasting regional discharge evolutions in the Amazon basin (1974–2004). J. Hydrol. 375, 297–311. https://doi.org/10.1016/j.jhydrol.2009.03.004.
Espinoza, J.C., Ronchail, J., Guyot, J.L., Junquas, C., Vauchel, P., Lavado, W., Drapeau, G., Pombosa, R., 2011. Climate variability and extreme drought in the upper Solimões River (western Amazon Basin): understanding the exceptional 2010 drought. Geophys. Res. Lett. 38 (13), L13406 https://doi.org/10.1029/2011GL047862.
Ferreira, B., da Cunha, F.F., Oliveira, R.A., Fernandes Filho, E.I., 2019. Estimation of reference evapotranspiration in Brazil with limited meteorological data using ANN and SVM – A new approach. J. Hydrol. 572, 556–570. https://doi.org/10.1016/j.jhydrol.2019.03.028.
GGWeather, 2023. Golden Gate Weather Services, 2023. El Niño and La Niña Years and Intensities, 2023) [WWW Document]. URL. https://ggweather.com/enso/oni.htm.
Gregory, N., Ewers, R.M., Chung, A.Y.C., Cator, L.J., 2019. El Niño drought and tropical forest conversion synergistically determine mosquito development rate. Environ. Res. Lett. 14, 035003 https://doi.org/10.1088/1748-9326/ab0036.
Holben, B.N., Eck, T.F., Slutsker, I., Tanré, D., Buis, J.P., Setzer, A., Vermote, E., Reagan, J.A., Kaufman, Y.J., Nakajima, T., Lavenu, F., Jankowiak, L., Smirnov, A., 1998. A federated instrument network and data archive for aerosol characterization. Remote Sens. Environ. 66, 1–16. https://doi.org/10.1016/S0034-4257(98)00031-5.
Jiménez-Muñoz, J., Mattar, C., Barichivich, J., Santamaría-Artigas, A., Takahashi, K., Malhi, Y., Sobrino, J.A., Schrier, G., 2016. Record-breaking warming and extreme drought in the Amazon rainforest during the course of El Niño 2015–2016. Sci. Rep. 6, 33130 https://doi.org/10.1038/srep.
Liu, S., Chen, M., Zhuang, Q., 2014. Aerosol effects on global land surface energy fluxes during 2003–2010. Geophys. Res. Lett. 41 (22), 7875–7881. https://doi.org/10.1002/2014GL061640.
Liu, Y., Brito, J., Dorris, M.R., Rivera-Rios, J.C., Seco, R., Bates, K.H., Artaxo, P., Duvoisin Jr., S., Keutsch, F.N., Kim, S., Goldstein, A.H., Guenther, A.B., Manzi, A.O., Souza, R.F.A., Springston, S.R., Watson, T.B., McKinney, K.A., Martin, S.T., 2016. Proc. Natl. Acad. Sci. USA 113 (22), 6125–6130. https://doi.org/10.1073/pnas.1524136113.
Lu, X., Chen, M., Liu, Y., Miralles, D.G., Wang, F., 2017. Enhanced water use efficiency in global terrestrial ecosystems under increasing aerosol loadings. Agric. For. Meteorol. 237–238, 39–49. https://doi.org/10.1016/j.agrformet.2017.02.002.
Lu, Z., Liu, Z., Zhu, J., Cobb, K.M., 2018. A review of paleo El Niño-southern oscillation. Atmosphere 9 (4), 130. https://doi.org/10.3390/atmos9040130.
Makarieva, A.M., Gorshkov, V.G., Sheil, D., Nobre, A.D., Li, B.L., 2013. Where do winds come from? A new theory on how water vapor condensation influences atmospheric pressure and dynamics. Atmos. Chem. Phys. 13, 1039–1056. https://doi.org/10.5194/acp-13-1039-2013.
Makarieva, A.M., Nefiodov, A.V., Nobre, A.D., Baudena, M., Bardi, U., Sheil, D., Saleska, S.R., Molina, R.D., Rammig, A., 2022. The role of ecosystem transpiration in creating alternate moisture regimes by influencing atmospheric moisture convergence. Global Change Biol. 29, 2536–2556. https://doi.org/10.1111/gcb.16644.
Marengo, J.A., Espinoza, J.C., 2016. Extreme seasonal droughts and floods in Amazonia: causes. trends and impacts. Int. J. Climatol. 36, 1033–1050. https://doi.org/10.1002/joc.4420.
Marengo, J.A., Alves, L.M., Soares, W.R., Rodriguez, D.A., Camargo, H., Riveros, M.P., Pabló, A.D., 2013. Two contrasting severe seasonal extremes in tropical south America in 2012: flood in amazonia and drought in Northeast Brazil. J. Clim. 26 (22), 9137–9154. https://doi.org/10.1175/JCLI-D-12-00642.1.
Marengo, J.A., Liebmann, B., Grimm, A.M., Misra, V., Silva Dias, P.L., Cavalcanti, I.F.A., Carvalho, L.M.V., Berbery, H., Ambrizzi, T., Vera, C.S., Saulo, A.C., Nogues Paegle, J., Zipser, E., Seth, A., Alves, L.M., 2012. Recent developments on the South American monsoon system. Int. J. Climatol. 32, 1–21. https://doi.org/10.1002/joc.2254.
Marengo, J.A., Tomasella, J., Alves, L.M., Soares, W., Rodriguez, D.A., 2011. The drought of 2010 in the context of historical droughts in the Amazon region. Geophys. Res. Lett. 38, 1–5. https://doi.org/10.1029/2011GL047436.
Marques, E.Q., Marimon-Junior, B.H., Marimon, B.S., Matricardi, E.A., Mews, H.A., Colli, G.R., 2020. Redefining the Cerrado–Amazonia transition: implications for conservation. Biodivers. Conserv. 29, 1501–1517. https://doi.org/10.1007/s10531-019-01720-z.
Menezes, J.A., Palácios, R.S., Junior, E.M.M., Junior, A.S., Nogueira, J.S., 2018. Caracterização espectral de propriedades ópticas de aerossóis em região de floresta tropical. Nativa 6, 451–456. https://doi.org/10.31413/nativa.v6i5.566.
Mishra, V., Cherkauer, K.A., 2010. Retrospective droughts in the crop growing season: implications to corn and soybean yield in the Midwestern United States. Agric. For. Meteorol. 150, 1030–1045. https://doi.org/10.1016/j.agrformet.2010.04.002.
Morais, F.G., Franco, M.A., Palácios, R., Machado, L.A.T., Rizzo, L.V., Barbosa, H.M.J., Jorge, F., Schafer, J.S., Holben, B.N., Landulfo, E., Artaxo, P., 2022. Relationship between land use and spatial variability of atmospheric Brown carbon and black carbon aerosols in Amazonia. Atmosphere 13, 1328. https://doi.org/10.3390/atmos13081328.
Moura, M.M., Santos, A.R., Pezzopane, J.E.M., Alexandre, R.S., Silva, S.F., Pimentel, S. M., Andrade, M.S.S., Silva, F.G.R., Branco, E.R.F., Moreira, T.R., Silva, R.G., Carvalho, J.R., 2019. Relation of El Niño and La Niña phenomena to precipitation, evapotranspiration and temperature in the Amazon basin. Sci. Total Environ. 651, 1639–1651. https://doi.org/10.1016/j.scitotenv.2018.09.242.
Nobre, C.A., Sampaio, G., Borma, L.S., Castilla-Rubio, J.C., Silva, J.S., Cardoso, M., 2016. Land-use and climate change risks in the Amazon and the need of a novel sustainable

development paradigm. Proc. Natl. Acad. Sci. USA 113, 10759–10768. https://doi.org/10.1073/pnas.1605516113.
Oliveira, B., Marimon Junior, B.H., Mews, H.A., Valadão, M.B.X., Marimon, B.S., 2017. Unraveling the ecosystem functions in the Amazonia–Cerrado transition: evidence of hyperdynamic nutrient cycling. Plant Ecol. 218, 225–239. https://doi.org/10.1007/s11258-016-0681-y.
Palácios, R., Romera, K., Rizzo, L., Cirino, G., Adams, D., Imbiriba, B., Nassarden, D., Rothmund, L., Siqueira, A., Basso, J., Rodrigues, T., Curado, L., Weber, A., Nogueira, J., Morais, F., Artaxo, P., 2022b. Atmos. Pollut. Res. 13, 101413 https://doi.org/10.1016/j.apr.2022.101413.
Palácios, R.S., Artaxo, P., Cirino, G.G., Nakale, V., Morais, F.G., Rothmund, L.D., Biudes, M.S., Machado, N.G., Curado, L.F.A., Marques, J.B., Nogueira, J., 2022a. Long-term measurements of aerosol optical properties and radiative forcing (2011-2017) over Central Amazonia. Atmósfera 35, 143–163. https://doi.org/10.20937/ATM.52892.
Palácios, R.S., de Paulo, S.R., de Paulo, I.J.C., Lobo, F.d.A., Maionchi, D.d.O., da Silva, H. J.A., da Silva, I.M.C.B., Marques, J.B., Biudes, M.S., Dalmagro, H.J., Rodrigues, T.R., Curado, L.F.A., 2023. Temporal evolution of vapor pressure deficit observed in six locations of different Brazilian ecosystems and its relationship with micrometeorological variables. Forests 14, 1543. https://doi.org/10.3390/f14081543.
Palácios, R.S., Romera, K.S., Curado, L.F.A., Banga, N.M., Rothmund, L.D., Sallo, F.S., Morais, D., Santos, A.C.A., Moraes, T.J., Morais, F.G., Landulfo, E., Franco, M.A.M., Kuhnen, I.A., Marques, J.B., Nogueira, J.S., Júnior, L.C.G.d.V., Rodrigues, T.R., 2020. Long term analysis of optical and radiative properties of aerosols in the Amazon basin. Aerosol Air Qual. Res. 20, 139–154. https://doi.org/10.4209/aaqr.2019.04.0189.
Pereira, A.G.C., Palácios, R., Santos, P.C.R., Pereira, R.V.S., Cirino, G., Imbiriba, B., 2024. Relationship between El niño-southern oscillation and atmospheric aerosols in the legal Amazon. Climate 12, 13. https://doi.org/10.3390/cli12020013.
Ponczek, M., Franco, M.A., Carbone, S., Rizzo, L.V., Santos, D.M., Morais, F.G., Duarte, A., Barbosa, H.M.J., Artaxo, P., 2022. Linking the chemical composition and optical properties of biomass burning aerosols in Amazonia. Environ. sci. Atmos. 2, 252–269. https://doi.org/10.1039/D1EA00055A.
Ramanathan, V., Crutzen, P.J., Kiehl, J.T., Rosenfeld, D., 2001. Aerosols, climate, and the hydrological cycle. Science 294 (5549), 2119–2124. https://doi.org/10.1126/science.1064034.
Sherwood, S., Fu, Q.A., 2014. Drier future? Science 343, 737–739. https://doi.org/10.1126/science.1247620.
Sousa, A.M.L., Rocha, E.J.P., Vitorino, M.I., Souza, P.J.O.P., Botelho, M.N., 2015. Variabilidade Espaço-Temporal da Precipitação na Amazônia Durante Eventos Enos. Rev. Bras. Geogr. Fís. 8, 13–24. https://doi.org/10.13140/RG.2.1.4123.2401.
Souza, A.P., Mota, L.L., Zamadei, T., Martim, C.C., Almeida, F.T., Paulino, J., 2013. Classificação climática e balanço hídrico climatológico no Estado de Mato Grosso. Nativa 1, 34–43. https://doi.org/10.31413/nativa.v1i1.1334, 2013.
Spontoni, T.A., Ventura, T.M., Palácios, R.S., Curado, L.F.A., Fernandes, W.A., Capistrano, V.B., Fritzen, C.L., Pavão, H.G., Rodrigues, T.R., 2023. Evaluation and modelling of reference evapotranspiration using different machine learning techniques for a Brazilian tropical savanna. Agronomy 13, 2056. https://doi.org/10.3390/agronomy13082056.
Valle Júnior, L.C.G., Ventura, T.M., Gomes, R.S.R., José de, S., Nogueira, J.S., Lobo, F.A., Vourlitis, G., Rodrigues, T.R., 2020. Comparative assessment of modelled and empirical reference evapotranspiration methods for a brazilian savanna. Agric. Water Manag. 232, 106040 https://doi.org/10.1016/j.agwat.2020.106040.
Valle Júnior, L.C.G.d., Vourlitis, G.L., Curado, L.F.A., Palácios, R.S., Nogueira, J.d.S., Lobo, F.d.A., Islam, A.R.M.T., Rodrigues, T.R., 2021. Evaluation of FAO-56 procedures for estimating reference evapotranspiration using missing climatic data for a Brazilian tropical savanna. Water 13, 1763. https://doi.org/10.3390/w13131763.
Verdan, I., Silva, M.E.S., 2022. South Atlantic convergence Zone variability in relation to ENSOevents from 2000 to 2021. R. Dep. Geografia 42, e193110. https://www.revistas.usp.br/rdg/article/view/193110/187515.
Vilanova, R.S., Delgado, R.C., Andrade, C.F., Santos, G.L., Magistrali, I.C., Oliveira, C.M. M., Teodoro, P.E., Capristo Silva, G.F., Silva Junior, C.A., Rodrigues, R.A., 2021. Vegetation degradation in ENSO events: drought assessment. soil use and vegetation evapotranspiration in the Western Brazilian Amazon. Remote Sens. Appl.: Soc. Environ. 23, 2352–9385. https://doi.org/10.1016/j.rsase.2021.100531.
Vourlitis, G.L., Lobo, F.A., Zeilhofer, P., Nogueira, J.S., 2011. Temporal patterns of net CO2 exchange for a tropical semideciduous forest of the southern Amazon Basin. J. Geophys. Res. Biogeosci. 116, G03029 https://doi.org/10.1029/2010JG001524.
Wang, B., Yue, X., Zhou, H., Zhu, J., 2022. Impact of diffuse radiation on evapotranspiration and its coupling to carbon fluxes at global FLUXNET sites. Agric. For. Meteorol. 322, 109006 https://doi.org/10.1016/j.agrformet.2022.109006.
WMO, 2014. 2014 - World Meteorological Organization. Guide to Meteorological Instruments and Methods of Observation. n.08. WMO, Geneva. Disponível em: http://www.posmet.ufv.br/wp-content/uploads/2016/09/MET-474-WMO-Guide.pdf.
Zamadei, T., Souza, A.P., Almeida, F.T., Escobedo, J.F., 2021. Daily Global and diffuse radiation in the Brazilian Cerrado-Amazon transition region. Cienc. Nat. 43, 1–20. https://doi.org/10.5902/2179460X39775.
Zhang, J., Ding, J., Zhang, J., Yuan, M., Li, P., Xiao, Z., Peng, C., Chen, H., Wang, M., Zhu, Q., 2020. Effects of increasing aerosol optical depth on the gross primary productivity in China during 2000–2014. Ecol. Indicat. 108, 105761 https://doi.org/10.1016/j.ecolind.2019.105761.
Zhang, K., Kimball, J., Nemani, R., Running, S.W., Hong, Y., Jonathan, J., Gourley, J.J., Yu, Z., 2015. Vegetation greening and climate change promote multidecadal rises of global land evapotranspiration. Sci. Rep. 5, 15956 https://doi.org/10.1038/srep15956.
Zhang, Li, L., Song, J., Akhter, Z.H., Zhang, J., 2023. Understanding aerosol–climate–ecosystem interactions and the implications for terrestrial carbon sink using the Community Earth System Model. Agric. For. Meteorol. 340, 109625 https://doi.org/10.1016/j.agrformet.2023.109625.
Zhang, Q., Manzoni, S., Katul, G., Porporato, A., Yang, D., 2014. The hysteretic evapotranspiration—vapor pressure deficit relation. J. Geophys. Res. Biogeosci. 119, 125–140. https://doi.org/10.1002/2013JG002484.
Zhang, Z., Liu, Q., Ruan, Y., Tan, Y., 2021. Estimation of aerosol radiative effects on terrestrial gross primary productivity and water use efficiency using process-based model and satellite data. Atmos. Res. 247 (2021), 105245 https://doi.org/10.1016/j.atmosres.2020.105245.
Zhou, H., Yue, X., Lei, Y., Chenguang Tian, C., Yimian Ma, Y., Cao, Y., 2021. Aerosol radiative and climatic effects on ecosystem productivity and evapotranspiration. Curr. Opin. Environ. Sci. Health. 19, 100218 https://doi.org/10.1016/j.coesh.2020.10.006.
Zhou, H., Yue, X., Lei, Y., Tian, C., Ma, Y., Cao, Y., 2022. Large contributions of diffuse radiation to global gross grimary productivity during 1981-2015 Glob. Biogeochem. Cycles. 35, e2021GB006957 https://doi.org/10.1029/2021GB006957.